Research Article | Vol. 12, No. 7 / 1 July 2021 / Biomedical Optics Express 3902
Biomedical Optics EXPRESS

Effects of photobiomodulation on the redox state of healthy and cancer cells

CLARA MARIA GONÇALVES DE FARIA,[1,*] HELOISA CIOL,[1] VANDERLEI SALVADOR BAGNATO,[1,2] AND SEBASTIÃO PRATAVIEIRA[1]

[1] São Carlos Institute of Physics - University of São Paulo, São Carlos, SP, Brazil
[2] Faculty Fellow at the Hagler Institute for Advanced Study and Visiting Professor at the Department of Biomedical Engineering - Texas A&M University, College Station Texas - USA 77843, USA
[*] claramgf@ifsc.usp.br

Abstract: Photobiomodulation therapy (PBMT) uses light to stimulate cells. The molecular basis of the effects of PBMT is being unveiled, but it is stated that the cytochrome-c oxidase enzyme in mitochondria, a photon acceptor of PBMT, contributes to an increase in ATP production and modulates the reduction and oxidation of electron carriers NADH and FAD. Since its effects are not fully understood, PBMT is not used on tumors. Thus, it is interesting to investigate if its effects correlate to mitochondrial metabolism and if so, how it could be linked to the optical redox ratio (ORR), defined as the ratio of FAD/(NADH + FAD) fluorescences. To that end, fibroblasts (HDFn cell line) and oral squamous cell carcinoma (SCC-25 cell line) were irradiated with a light source of 780 nm and a total dose of 5 J/cm^2, and imaged by optical microscopy. PBMT down-regulated the SCC-25 ORR by 10%. Furthermore, PBMT led to an increase in ROS and ATP production in carcinoma cells after 4 h, while fibroblasts only had a modest ATP increase 6 h after irradiation. Cell lines did not show distinct cell cycle profiles, as both had an increase in G2/M cells. This study indicates that PBMT decreases the redox state of oral cancer by possibly increasing glycolysis and affects normal and tumor cells through distinct pathways. To our knowledge, this is the first study that investigated the effects of PBMT on mitochondrial metabolism from the initiation of the cascade to DNA replication. This is an essential step in the investigation of the mechanism of action of PBMT in an effort to avoid misinterpretations of a variety of combined protocols.

1. Introduction

Photobiomodulation therapy (PBMT) has been used for decades for wound healing, tissue regeneration, analgesia, inflammation reduction, osteoarthritis, reducing edema on lymph nodes, and muscle relaxation, among others [1,2]. However, it is a developing field which results in partial acceptance and recognition from authorities in biomedical science, professionals and scholarly journals [3]. It encompasses a variety of reactions caused by non-ionizing and non-thermal light absorption in tissues and cells, resulting in a physiological response according to tissue stimulation. However, its effects are still unclear, particularly on premalignant and malignant cells. One of PBMT most popular applications, due to its effectiveness, is the prevention and management of oral mucositis in head and neck squamous cell carcinoma (HNSCC) patients [4,5]. Still, a recent systematic review, including 13 papers, demonstrated that the data does not support a definite conclusion of photobiomodulation (PBM) impact on HNSCC cells, despite many studies on the topic [4]. Among the challenges are the wide variety of study designs, PBMT protocols and the limited type of assays performed, where cell proliferation and viability are the primary ones.

Evidence indicates that the PBM cascade of events begins with cytochrome c oxidase (COX), the fourth protein complex in the mitochondrial electron transport chain and primary photoreceptor

#421302 https://doi.org/10.1364/BOE.421302
Journal © 2021 Received 1 Feb 2021; revised 9 Apr 2021; accepted 29 Apr 2021; published 8 Jun 2021

Biomedical Optics EXPRESS

of red and near-infrared light [6–8]. The energy absorbed by COX changes the mitochondrial potential and leads to up or downregulation of reactive oxygen species (ROS), adenosine triphosphate (ATP) [9], [3] and calcium (Ca^{2+}) [1]. These molecules trigger the activation of transcription factors (e.g., NF-κB, Nrf2 and activator protein-1[AP-1]) [10], changes in protein expression and release of cytokines and growth factors [11]. The exact effects that follows are hard to predict: it includes altered mitochondrial activity [12], gene expression [1,13,14], promotion of anti-inflammatory response [3] and cell proliferation [15]. ROS, for example, leads to apoptosis, if found in great amounts, and may also increase proliferation at lower levels. Therefore, investigating the modulation of these molecules activity by PBM and its connection with changes in metabolism and physiological effects, within the same conditions of illumination and cell type, is fundamental.

Glucose is the primary fuel of cellular respiration; its catabolism reduces the electron carriers by transferring electrons to FAD molecules, producing $FADH_2$ and NAD coenzymes, providing NADH [16]. The NADH and $FADH_2$ are oxidized, respectively, to NAD^+ and FAD at complexes I and II of the electron transport chain, producing an electrical potential that results in a donation of electrons to molecular oxygen and phosphorylation of adenosine diphosphate (ADP) by the ATP synthase enzyme [17]. Generally, lower oxygen concentrations shift the glucose catabolism to anaerobic glycolysis, which converts glucose to lactate instead of pyruvate, supplying enough energy for the maintenance of cellular processes [18]. The glycolytic pathway takes place at the cytosol resulting in ATP generation and oxidation of phosphoenolpyruvate to pyruvate.

In non-cancer cells, this pathway can either provide enough energy to cells under hypoxic conditions or supply the citric acid cycle with pyruvate to produce mitochondrial ATP by oxidative phosphorylation (OXPHOS) [19]. The formed NADH and FAD of these coenzymes present an intrinsic fluorescence, which allows the redox ratio (RR) of the cell to be calculated optically by FAD/ [NADH + FAD] fluorescence intensities [17,20,21]. The optical redox ratio (ORR) is proportional to the balance of oxidative phosphorylation/glycolysis and can be used to monitor living tissues and cells (Fig. 1) [22]. Several conditions change cellular metabolism and alter this balance, such as hypoxia, high carbon demands, increased proliferation rate, and fatty acid synthesis [21]. The ORR is also used to investigate cancer mechanisms since different types of tumors, and cancer cells favor glycolysis over OXPHOS, even in the presence of oxygen, a phenomenon called ”Warburg effect” or aerobic glycolysis [23]. Choosing aerobic glycolysis could benefit cancer cells by supplying ATP faster than oxidative phosphorylation [24] and by going through an energetic pathway that produces lower concentrations of ROS [17]. It must be stated that cancer cells can favor oxidative metabolism over aerobic glycolysis, for reasons not fully elucidated. Highly invasive tumor cells, for example, have shown modulation of the glucose metabolic pathway depending on the site of metastasis [25–27]. Oral cancer is one of them, and its location is convenient to make optical measurements and an ORR analysis. Previous studies have shown that it is possible to differentiate healthy tissue, hyperplasia, and dysplasia with this technique *in vivo*, which shows its potential to monitor metabolism changes in the tumor [28].

Therefore, in order to increase PBMT acceptance, it is fundamental to investigate its effects on the metabolism of cancer cells, since it is a modality clinically used to treat and prevent side effects, such as mucositis, in cancer patients undergoing radio and chemotherapy. To do so, PBMT mechanisms on oral cancer and normal tissue must be known. Despite studies on the activation of a few pathways and the regulation of important molecules alone do exist, the overall PBMT effect on metabolism or the existing correlations among them have not been clearly identified or understood [21]. Thus, the aims of this study were to explore PBM effects on ORR and its correlation with the cell cycle, ATP levels, and ROS production, and to elucidate PBM effects related to the activation of biochemical carriers and the overall impact on the metabolism of oral cancer cells and fibroblasts, which play an important role in normal tissue regeneration, including mucositis regeneration.

Biomedical Optics EXPRESS

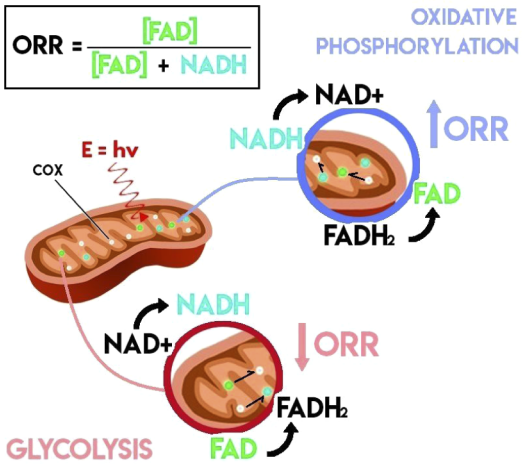

Fig. 1. Schematics of the optical redox ratio (ORR) in mitochondria, following light absorption by cytochrome c oxidase (COX), and its correlation to the ATP generation pathway. Normal cells produce ATP by oxidative phosphorylation (OXPHOS) in normoxic conditions. Within the mitochondria, NADH and $FADH_2$ are oxidized, respectively, to NAD^+ and FAD, increasing RR. In hypoxic conditions, cells use the glycolysis pathway to supply ATP. Glycolysis reduces the electron carriers NAD^+ and FAD to NADH and $FADH_2$, respectively, lowering the ORR.

2. Material and methods

2.1. Cell culture

Human dermal fibroblasts neonatal (HDFn) and squamous carcinoma SCC-25 (American Type Culture Collection - ATCC), Wesel, Germany), were cultivated at 37∘C in humidified 5% CO_2 atmosphere in Dulbecco's modified Eagle medium (DMEM) and DMEM/Ham's (Cultilab), respectively. Media were supplemented with 10% (v/v) Fetal Bovine Serum (Cultilab, Brazil) and to DMEM/Ham's hydrocortisone was added (Sigma-Aldrich, USA) at a concentration of 400 ng/ml. Cells were used at maximum passage of 20 and tested negatice for mycoplasma prior the experiments.

2.2. Illumination protocol

PBMT groups were illuminated using a custom-made LED array device (Figure S1, Supplement 1) emitting at 780 nm with an irradiance of 30 mW/cm^2 and a total fluence rate of 5 J/cm^2, given in 2 min and 53 s at room temperature. [29] The control groups were sham treated. A flow chart of all analysis performed after PBM is shown in Figure S2 (Supplement 1).

2.3. Optical redox ratio imaging

Cells were plated on a 35 mm glass bottom dish (Greiner Bio-One, Germany) at a density of 5 x 10^5 cells and let in a heated chamber (37°C, 5%, CO_2) overnight. Four hours after PBMT, cells were washed twice in PBS and maintained in the buffer for image acquisition, perfomed on an inverted fluorescence confocal microscope (Zeiss - LSM780, Zeiss, Germany) equipped with a Ti:Sapphire tunable laser source (Chameleon Vision II, Coherent Inc., USA), using the multiphoton modality of two-photon absorption induced fluorescence. The laser excitation source was tuned to 755 nm (NADH excitation, 300 mW at the sample) or 860 nm (FAD excitation, 600 mW at the sample), and images were acquired in the channel mode of the microscope with

Biomedical Optics EXPRESS

440 - 480 nm (NADH fluorescence) or 500 - 550 nm (FAD fluorescence) wavelength range, respectively (1.58 μs dwell time, 2 line/frame averaging). Images (1024 x 1024 pixels; 8-bit depth; 425 μm x 425 μm) were acquired using a 20x objective (NA = 0.8). For each condition, two plates were prepared and 10 fields were imaged for each one. Three independent experiments were performed (n=3). To calculate cell-to-cell ORR heterogeneity, a region of interest (ROI) was selected and used to create a mask to compute the mean ORR of a single cell. The mask was created manually from the FAD image. Three cells of each field were analyzed, resulting in the analysis of 120 cells per group, from three independent dishes (n=3). To ensure that the same dish would yield the same result, two dishes were calculated twice, using different cells from the field. Then, the 'heterogeneity', defined as the ratio of standard deviation/mean ORR, was calculated for each dish. Therefore, the error bar of this parameter represents the standard deviation of the heterogeneity value of three dishes. All images were acquired using Zen 2010 software (Zeiss, Germany). Laser power was checked daily to ensure its value was approximately the same at all experimnt-days. Additionally, a control plate was imaged as the standard, in order to compare its value among the different days and account for daily system fluctuations. Image analysis was performed using MATLAB (MathWorks, USA), thresholding was performed by removing pixels with NAD+FAD < 0.4 to eliminate background and contribution from other chromophores, such as keratin. The latter results in pixels with a high intensity in one channel but a low one on the other. This approach was validated by analysing the isolated contributions from the removed pixels for all conditions, and concluding that their contribution was minor and uniform along the groups. Redox images and their mean values were created by computing pixel-wise ratios of FAD/(NADH + FAD) fluorescence. For statistical analysis and bar plot presentation, the average redox ratios of each group were calculated by separately computing the means from their respective images.

2.4. Glycolysis assay

Glycolysis was assessed with a fluorescent kit (Abcam ab197244, Abcam, USA) following manufacturer protocols. $2x10^4$ cells/well were seeded in 96-well opaque black walls 24 h prior illumination, in 6 replicates per group. Then, 1h after PBMT, CO_2 was removed from the incubator and at 4h after PBMT wells were washed twice with Respiration Buffer and 15 μl of Glycolysis assay reagent in 100 μl of Buffer was added to each well. Fluorescence (ex/em: 380/615 nm) was measured with a SpectraMax M5 Multi-Mode Microplate Reader (Molecular Devices, USA) for 2h in 1.5 min intervals. The means correspond to two independent experiments (n=2).

2.5. Metabolic activity assessment by MTT assay

Metabolic activity was assessed at 4h and 24h after PBMT. Cells were seeded in triplicate for each condition in 24-wells plates at a density of $1x10^5$ per well (500 μl) and illuminated in culture medium the following day according to the parameters mentioned above. After 4h or 24h, medium was replaced by 250 μl of new media with 3-(4,5-dimethylthiazol-2-yl)-2,5-diphenyltetrazolium bromide (MTT) (5 μg/ml) and incubated for 3h, until 1 ml of DMSO was added and absorbance was measured at 570 nm in a microplate reader (Multiskan™ FC Microplate Photometer - ThermoFisher Scientific, USA). Each experiment was performed three independent times (n=3). To confirm whether the results from MTT resulted proliferation and viability, a trypan blue exclusion assay was performed in quadruplicate, in the same conditions.

2.6. ROS assay

Quantification of ROS after PBMT was performed by flow cytometry assessment using DCFH-DA. For the assay, a 1×10^6 cells per ml suspension was made in phenol and FBS free medium. Triplicates of 250 μl of the cell suspension were illuminated in a 24-wells plate with a dose

Biomedical Optics EXPRESS

of 5 J/cm^2 at 780 nm in a black 24-wells plate with clear bottom. Samples were immediately incubated with 250 μl of DCFDA solution, resulting in a concentration of 25 μM, for 30 minutes at room temperature in the dark and assessed by flow cytometry (BD, C6 Accuri Plus, USA) at an excitation/emission of 492-495 nm/517-527 nm.

2.7. ATP assay

Cells were seeded in 96-well plates at a 2x10^4 cells/well density and incubated at 37°C, 5% CO_2 for 24h prior the ATP assay, performed with the ATP bioluminescent assay kit (Sigma-Aldrich, USA). Plates were illuminated or sham-illuminated in medium and at a specific time after that ranged from 1-24h supernatant was removed, wells were washed twice with PBS and 100 μl of Releasing Reagent were added. The working solution was prepared as indicated (10% of ATP Mix Working Solution in ATP Mix Dilution Buffer). Immediately prior to the bioluminescent reading, 100 μl was added to the wells with a multi-channel pipette to ensure all wells were incubated simultaneously and only 6 wells were read at a time. The luminescence was measured with a SpectraMax M5 Multi-Mode Microplate Reader (Molecular Devices, USA). Experiments were repeated three times with 6 replicates per group (n=3).

2.8. Cell cycle assessment

Cell cycle evaluation was performed by flow cytometry analysis using propidium iodide (PI). Cells were seeded in 24-wells plate and illuminated in culture medium as described previously, in triplicate. Then, at 0h, 8h and 24h after illumination, cells were collected and fixed in ice-cold 70 % ethanol at -20°C for at least 24 h, then washed with PBS and stained with PI (50 μg PI/ml in PBS, BD Biosciences) containing 0.1 mg/ml RNase (Sigma-Aldrich, USA) for 40 min. Samples were analyzed in an Accuri C6 flow cytometer (BD Biosciences, USA) in triplicate and cell cycle was determined using FlowJo software univariate analysis (BD Biosciences, USA). Two independent experiments were performed (n=2). Representative histograms of each group, showing the estimated areas of the cell cycle stages, are shown in Figure S3 (Supplement 1).

2.9. Statistical analysis

The data were plotted using boxplot with a whisker of 1-99 or represented as means ± standard deviation and were analyzed using the commercially available software Origin 2018 (Origin Lab., USA). One-way analysis of variance (ANOVA) was used among the categories “HDFn” and “SCC-25" cells and “Control" and “PBM" for the ORR measurements. For experiments that we compared only “PBM" and “Control" independently for the same cell line, a single ANOVA test was performed. Differences were considered as statistically significant at $p<0.05$. Asterisks placed above bars indicate statistical significance.

3. Results

3.1. Optical redox ratio imaging

For imaging, two-photons excitation fluorescence (TPEF) microscopy allowed the acquisition of high resolution images of depth sectioning without the need for a confocal pinhole, since TPEF is a non-linear light process limited to the focal plane, which also spares any damage to surrounding tissue or cells [21,30]. Figure 2 shows the NADH (blue) and FAD (green) fluorescence by TPEF microscopy and the merged image (red) indicating the ORR of the SCC-25 cells (Fig. 2(a)-(c)) and HDFn (Fig. 2(d)-(f)).

From the results shown in Fig. 2(g), it is evident that HDFn fibroblasts present a higher ORR than SCC-25 carcinoma cells. This is rational since normal cells favor oxidative phosphorylation (↑FAD/(↑FAD+↓NADH)) over glycolysis (↓FAD/(↓FAD+↑NADH)) and is consistent with previous observations [17,21]. Regarding PBMT, illumination did not show a significant effect on

Biomedical Optics EXPRESS

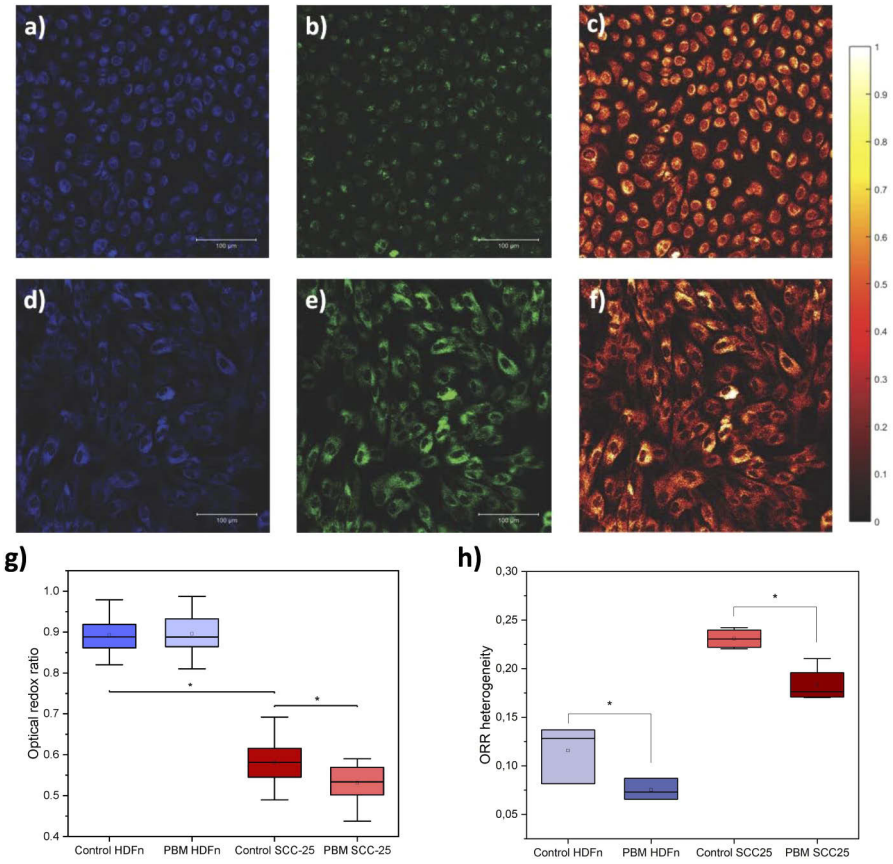

Fig. 2. Fluorescence microscopy of SCC-25 (a-c) and HDFn (d-f) cells. The false color blue images (a and d) correspond to NADH fluorescence, false color green (b and e) correspond to FAD fluorescence and the false color red (c and f) are the calculated optical redox ratio image. (g) Mean optical redox ratio of HDFn and SCC-25 cells, control and PBM groups (n=3, * indicates $p < 0.01$). (h) Cell-to-cell relative heterogeneity in the redox ratio for SCC-25 and HDFn cells, control and PBM (n=3, * indicates $p < 0.05$).

HFDn ORR value, however, it decreased the ratio of SCC-25 cells by 10%, indicating increased glucose catabolism. Additionally, cell-to-cell ORR heterogeneity was calculated using a region of interest (ROI) mask to compute the mean redox ratio of a single cell. It is noticeable that the heterogeneity shown is greater for SCC-25 cells than for healthy HDFn cells. This is consistent with the fact that some tumor cells, presenting a more metastatic potential, contradict the Warburg effect, [17] which consists in the preferential metabolism of glucose to lactate, independent of oxygen presence, by cancer cells [31]. Another interesting observation is that PBM reduced the heterogeneity in both cell lines (2(f)), despite not causing a difference in the ORR mean of HDFn cells. This means that the balance of oxidative phosphorylation/glycolysis among the population became more homogeneous after illumination. If we combine this result with the decrease in the mean of SCC-25 ORR, it is possible to raise the hypothesis that PBM induces an upregulation of glucose catabolism compared to OXPHOS. For HDFn cells, the decrease in heterogeneity could be related to PBM producing slightly different effects according to the state of a cell, upregulating OXPHOS in cells presenting a lower redox state and decreasing glycolysis in the ones that favored it instead of OXPHOS.

Biomedical Optics EXPRESS

3.2. Glycolysis

Glycolysis results after 4 hr of PBMT are shown in Fig. 3. It is seen in Fig. 3(a) that fibroblasts present a lower baseline for glycolysis than the tumor cell line, as expected due to the Warburg effect observed in cancer cells. The PBMT caused an increase in this parameter in both cell lines (Fig. 3(b) and 3(c)), in a similar proportion. As HDFn cells did not present a difference in ORR after PBMT we conclude that OXPHOS increased as well, and the balance was not altered. The SCC-25 cells showed a decrease in ORR and an increase in glycolysis, making it possible to infer that OXPHOS had either a smaller increase than glycolysis, was not affected, or had a slight decrease.

3.3. MTT assay

Cell viability was assessed by the Metabolic activity assessment by 3-(4,5-dimethylthiazol-2-yl)-2,5-diphenyltetrazolium bromide (MTT) assay 4 h and 24 h after PBMT and is shown in Fig. 4. Since this assay is used to measure cell viability based on cell metabolism, cell counting was performed to confirm the results from MTT and showed a good correlation (see SI). Thus, the first time point was chosen to investigate metabolic changes only, while 24 h allows the visualization of viability and different cell numbers as well. Earlier times were not investigated since PBM effects take a few hours to result in metabolic alterations. In the results, it is possible to observe a difference in cell viability 4 h after PBMT in both cell lines alongside similar cell counting, which indicates a change in metabolism in both cells. Mitochondrial activity was increased in fibroblasts (Fig. 4(a)) and decreased in SCC-25 cells (Fig. 4(b)). At 24 h, it was observed that PBM induced proliferation in fibroblasts, as both MTT and cell counting increased. However, there was no significant change in the tumor population.

3.4. ROS and ATP assay

The ROS quantification after PBMT was performed by flow cytometry to investigate if its production correlated to illumination (Fig. 5). Figure 5(a) shows the ratio of mean intensities between PBMT and the control of each cell line. In fibroblasts, no significant ($p > 0.05$) changes were found among the samples. In SCC-25, however, a statistically significant ($p < 0.05$) increase of about 30% was observed after PBMT. This suggests that ROS could play an important role in mediating PBM effects in tumor cells but not in normal fibroblasts. One common consequence of several pathways initiated by ROS is increased ATP production. As seen in Fig. 5(b), endogenous ATP increased within the 24 h-after PBMT period evaluated for SCC-25 and HDFn cells, even though kinetics differed among the cell lines. SCC-25 cells presented a peak of 1.25 units compared to the control at 4 h after PBMT while fibroblasts modestly increased ATP by 7 % 6 h after PBMT. Interestingly, both cells showed a decrease immediately after its ATP peaks, indicating consumption by energy demanding processes.

3.5. Cell cycle assessment

Cell cycle was evaluated by flow cytometry 8 h and 24 h after PBMT or sham treatment. The proportion of cells in G2/M after PBMT relative to the control is shown in Fig. 6. Cells in G0/G1 and S phase were not statistically different. It was observed that both fibroblast and tumor cells increased mitosis in a linear manner and at the same rate, reaching a 20 % increase in 24 h.

Biomedical Optics EXPRESS

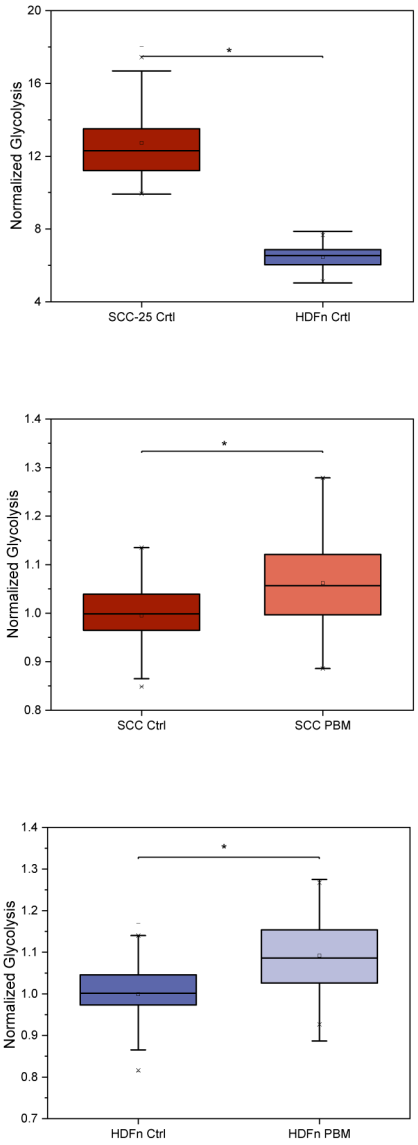

Fig. 3. Glycolysis experiment assay. (a) Baseline of glycolysis for SCC-25 and HDFn cell line showing that the tumor cell line (SCC-25) has a greater baseline for glycolysis when compared to HDFn cells. This result was expected and could be related to the Warburg effect. (b) Glycolysis quantification after PBMT for SCC-25 cell line and (c) for HDFn cell line. Results show that PBM did not influence the glycolysis rate of normal cells but increased the rate of tumor cells. $^{*}p < 0.05$

Biomedical Optics EXPRESS

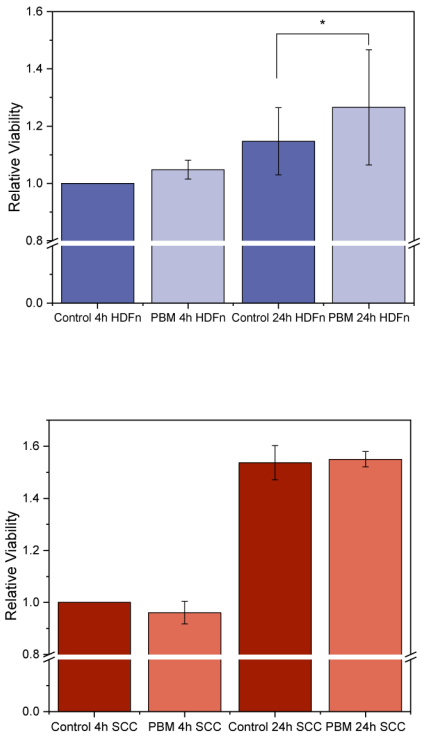

Fig. 4. Metabolic activity by MTT assay 4 h and 24 h after PBMT. (a) shows the HDFn cell line viability of control samples and illuminated samples, indicating that PBM induced cell proliferation in fibroblasts after 24 h. (b) Cell viability assay for SCC-25 cells. When compared to control, no cell proliferation was observed in tumor line 24 h after illumination.

Biomedical Optics EXPRESS

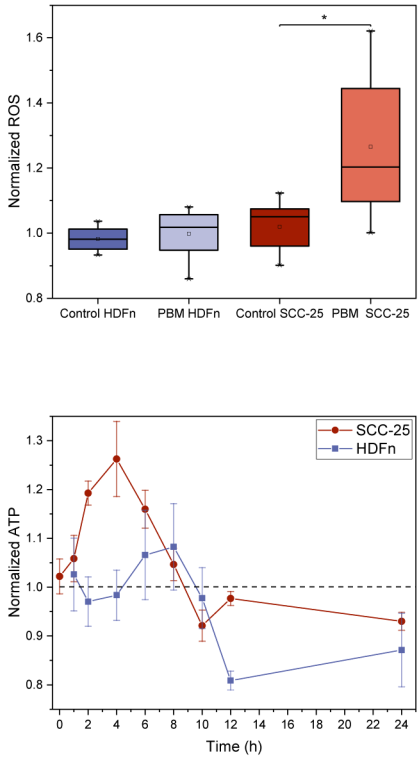

Fig. 5. ROS and ATP assay. (a) The ROS production assay indicating that PBM induced ROS production in the SCC-25 cell line ($p < 0.05$), but not in fibroblasts. (b) The ATP production of both cell lines, indicating that SCC-25 (red-dot) cells increased a peak of 1.25 units 4 h after PBMT, as fibroblasts modestly increased 7 % after 6 h (grey-square).

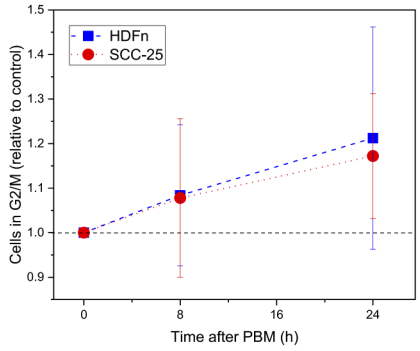

Fig. 6. Cell cycle assessment by flow cytometry. Illuminated samples of HDFn (blue-square line) and SCC-25 (red-dot line) linearly increased the mitosis rate up to 20% after 24 h when compared to controls.

Biomedical Optics EXPRESS

4. Discussion

Photobiomodulation is the use of light, mainly in the red and near-infrared regions, for a variety of purposes. It is promising since it is a non-invasive and an affordable technique already used to reduce inflammatory conditions [3], in the treatment of arthritis [32] and wound healing [33], among others, resulting in pain relief and modulation of expression of genes related to the inflammatory response [6,34,35]. The PBMT encompasses such a broad spectrum of illumination protocols, parameters, and uses; its mechanism of action is not fully understood. This causes skepticism from the medical community and limits its impact. As stated by Stephen Sonis [36], until we obtain enough data we cannot answer whether we should avoid PBMT in head and neck cancer tumors or not. So it is fundamental to understand these effects to ensure the safety of this technique and explore its potential in enhancing cancer treatment.

In this study, we investigated the effects of PBM on the metabolism of healthy (HDFn) and cancer cells (SCC-25) *in vitro* and revealed that their pathways are different. It was also established that ORR evaluation by TPEF is a technique that is sensitive enough to significantly detect slight changes caused by PBM. Thus, it is a powerful tool to investigate metabolism modulation in both cancer and normal cells. The PBMT illumination protocol was based on previous mucositis studies [37,38] and the results are summarized in Fig. 7. In fibroblasts cells, no changes in the redox state were observed 4 h after illumination despite increased glycolysis displayed by a different method. Therefore, both forms of respiration might have increased at the same rate in these cells, maintaining the ratio constant. In SCC-25 cells, a lower ORR after PBM indicates a possible increase of glycolysis compared to OXPHOS. Nevertheless, there are other process that affect the redox state of the cells, such as glutaminolysis, fatty acid oxidation/synthesis and apoptosis, so further studies are needed to confirm this hypothesis [39,40].

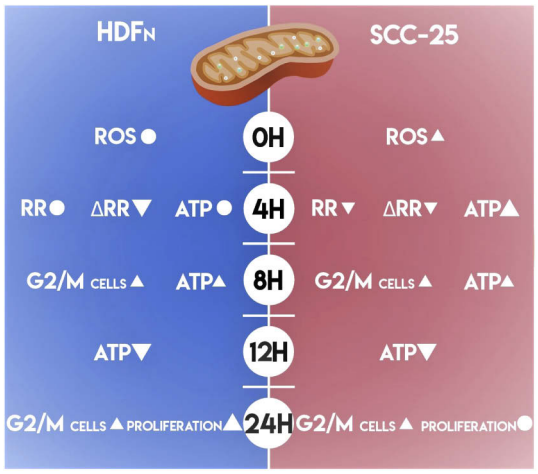

Fig. 7. Summary of HDFn and SCC-25 modulations caused by PBM indicating increase, decrease or no change in reactive oxygen species (ROS), redox ratio (RR), redox ratio heterogeneity (ΔRR), adenosine triphosphate (ATP), number of cells in G2/M and proliferation, compared to its respective controls.

Previous work by Heymann and colleagues reported a PBM-induced decrease in the redox ratio, measured by the extracellular flux assay, along with increased proliferation in HeLa cells, using 670 nm and 12 J/cm^2 [41]. Since the illumination protocol and cell type were different, but the effect similar, it might be a common effect of PBM in tumors. Its consequences in cancer cells need to be investigated since it may correlate to the Warburg effect and its therapeutic implications, such as tumor aggressiveness shown by Li et. al. [42].

Biomedical Optics EXPRESS

Additional evidence that arose from the ORR analysis is that PBM may have different effects and mechanism of action depending on the previous redox state of the cells. This was shown by decreased heterogeneity in ORR values 4 h after illumination, in both cell lines, caused by a decrease in the highest and an increase in the lowest values of ORR. It suggests that PBM acts differently according to the cells. In this instance, it may be more effective to the ones that differ from the mean redox state of the population.

Beyond the differences in ORR, fibroblasts and SCC-25 cells, these seem to have distinguished pathways that initiate the cascade of events that characterize PBM. ROS is known to be an important biomarker that induces apoptosis if found in high concentrations, and modulates pro-survival and proliferation effects at low concentrations [43]. In this study, ROS concentration increased only in SCC-25 cells, indicating that PBM acts by a different pathway in fibroblasts. Engel and colleagues showed increased catalase in fibroblasts after PBM scavenged ROS. Therefore, they suggested that lineage-specific differences maintain homeostatic redox status within each cell type [43]. Lunova et al. have stressed how PBM mechanisms are complex by showing that blue and red light cause opposite changes in the mitochondrial potential by exciting different structures in COX [44]. Lynnyk et al. have demonstrated that different doses of laser irradiation result in distinct biochemical signaling, which may be initiated by different intracellular ROS compartmentalization [45].

Nevertheless, ATP levels were increased in both cell lines after PBMT. Chen et. al. showed in fibroblasts, that ATP increase after PBM is not altered with the addition of antioxidants. Despite showing an increase in ROS that was not seen in our study, both results suggest that ATP synthesis after PBMT is not dependent on ROS signaling [46]. ATP kinetics after PBMT, however, have not been investigated yet. Such an investigation is important because end-point measurements can lead to false conclusions. For example, ATP increase in fibroblasts was only seen 8 h after PBMT while its peak for SCC-25 cells was seen at 4 h. At 12 h, ATP levels were lower when compared to the non-illuminated groups for both cells lines. This indicates higher ATP demands from processes induced by PBM, such as protein synthesis and DNA replication involved in proliferation, or a mechanism of feedback that tends to suppress the effects caused by light.

In fact, we observed an increase in G2/M fraction for both cells at 8 and 12 h after PBMT. However, it did not result in increased proliferation in the tumor cell line but did in HDFn cells. This is an encouraging result that supports the evidence that PBM does not affect tumor growth [47]. Schartinger et al. reported similar results using 660 nm, an increase in fibroblasts but a decrease in SCC-25 cells [48]. This indicates regarding proliferation, that PBM effects are similar for multiple wavelengths. Regarding cell cycle, they observed an increase fraction in cell cycle G1 and S phases, but did not report the time after PBMT in which the measurement was performed. In contrast, Sperandio et al. observed increased proliferation in SCC-25 cells for both 660 and 780 nm, at 24 h (780 nm, 6.15 J/cm^2) and 48 h (660 and 780 nm, 3.07 J/cm^2) after illumination [49]. Certainly, further studies need to be conducted to understand if PBM stimulates proliferation in tumors, and under what conditions, in order to advance the reliability and security of its applications in cancer.

Therefore, it was demonstrated that PBMT with 5 J/cm^2 at 780 nm alters the metabolism of fibroblasts and HNSCC cells, but in different pathways and kinetics. Its mechanism of action needs to be further investigated to improve the understanding of these differences. For that, studies in more complex models, 3D cell cultures and *in vivo*, need to be conducted. So the influence of the extracellular matrix, spatial fluence distribution, surrounding tissues, immune and vascular response, among others, can be evaluated. Then, it may be possible to explore PBM mechanisms to improve cancer treatments, or avoid applications involving tumors to prevent negative effects. Additionally, TPEF was depicted as a powerful tool to evaluate redox state after PBMT. It is a sensitive technique that allows the assessment of small redox ratio differences and heterogeneity

Biomedical Optics EXPRESS

among cells. It is also nondestructive, so the sample can be used after measurements, and it can be combined with other fluorescent markers.

Funding. Conselho Nacional de Desenvolvimento Científico e Tecnológico (306919/2019-2, 465360/2014-9); Fundação de Amparo à Pesquisa do Estado de São Paulo (2009/54035-4, 2013/07276-1, 2014/50857-8, 2017/14182-4).

Acknowledgments. The authors thank Camila Bramorski and André Longo for the support with the figures and acknowledge the support provided by Brazilian Funding Agencies: Coordenação de Aperfeiçoamento de Pessoal de Nível Superior - Brasil (CAPES) - Finance Code 001; CNPq (465360/2014-9 and 306919/2019-2) and São Paulo Research Foundation (FAPESP) grants: 2009/54035-4 (EMU); 2013/07276-1 (CePOF); 2014/50857-8 (INCT); 2017/14182-4 (CMGF scholarship).

Disclosures. The authors declare no conflicts of interest.

Data Availability. Data underlying the results presented in this paper are available in Dataset 1 [50].

Supplemental document. See Supplement 1 for supporting content.

References

1. L. F. de Freitas and M. R. Hamblin, "Proposed mechanisms of photobiomodulation or low-level light therapy," IEEE J. Sel. Top. Quantum Electron. **22**(3), 348–364 (2016).
2. T. Karu, "Is it time to consider photobiomodulation as a drug equivalent?" Photomed. Laser Surg. **31**(5), 189–191 (2013).
3. M. R. Hamblin, "Mechanisms and applications of the anti-inflammatory effects of photobiomodulation," AIMS Biophys. **4**(3), 337–361 (2017).
4. F. M. Silveira, M. d. P. Paglioni, M. M. Marques, A. R. Santos-Silva, C. A. Migliorati, P. Arany, and M. D. Martins, "Examining tumor modulating effects of photobiomodulation therapy on head and neck squamous cell carcinomas," Photochem. Photobiol. Sci. **18**(7), 1621–1637 (2019).
5. Y. Zadik, P. R. Arany, E. R. Fregnani, P. Bossi, H. S. Antunes, R.-J. Bensadoun, L. A. Gueiros, A. Majorana, R. G. Nair, V. Ranna, W. J. E. Tissing, A. Vaddi, R. Lubart, C. A. Migliorati, R. V. Lalla, K. K. F. Cheng, and S. Elad, and On behalf of The Mucositis Study Group of the Multinational Association of Supportive Care in Cancer/International Society of Oral Oncology (MASCC/ISOO), "Systematic review of photobiomodulation for the management of oral mucositis in cancer patients and clinical practice guidelines," Support. Care Cancer **27**(10), 3969–3983 (2019).
6. A. C.-H. Chen, P. R. Arany, Y.-Y. Huang, E. M. Tomkinson, S. K. Sharma, G. B. Kharkwal, T. Saleem, D. Mooney, F. E. Yull, T. S. Blackwell, and M. R. Hamblin, "Low-level laser therapy activates NF-kB via generation of reactive oxygen species in mouse embryonic fibroblasts," PLoS One **6**(7), e22453 (2011).
7. T. Karu, "Mitochondrial mechanisms of photobiomodulation in context of new data about multiple roles of ATP," Photomed. Laser Surg. **28**(2), 159–160 (2010).
8. D. Pastore, M. Greco, and S. Passarella, "Specific helium-neon laser sensitivity of the purified cytochrome c oxidase," Int. J. Radiat. Biol. **76**(6), 863–870 (2000).
9. C. Ferraresi, B. Kaippert, P. Avci, Y.-Y. Huang, M. V. P. de Sousa, V. S. Bagnato, N. A. Parizotto, and M. R. Hamblin, "Low-level laser (light) therapy increases mitochondrial membrane potential and ATP synthesis in C2c12 myotubes with a peak response at 3-6 hours," Photochem. Photobiol. **91**(2), 411–416 (2015).
10. P. R. Arany, A. Cho, T. D. Hunt, G. Sidhu, K. Shin, E. Hahm, G. X. Huang, J. Weaver, A. C.-H. Chen, B. L. Padwa, M. R. Hamblin, M. H. Barcellos-Hoff, A. B. Kulkarni, and D. J Mooney, "Photoactivation of endogenous latent transforming growth factor-β1 directs dental stem cell differentiation for regeneration," Sci. Transl. Med. **6**(238), 238ra69 (2014).
11. J. T. Eells, M. M. Henry, P. Summerfelt, M. T. T. Wong-Riley, E. V. Buchmann, M. Kane, N. T. Whelan, and H. T. Whelan, "Therapeutic photobiomodulation for methanol-induced retinal toxicity," Proc. Natl. Acad. Sci. U. S. A. **100**(6), 3439–3444 (2003).
12. T. I. Karu, "Multiple roles of cytochrome c oxidase in mammalian cells under action of red and IR-A radiation," IUBMB Life **62**(8), 607–610 (2010).
13. K. R. Byrnes, X. Wu, R. W. Waynant, I. K. Ilev, and J. J. Anders, "Low power laser irradiation alters gene expression of olfactory ensheathing cells in vitro," Lasers Surg. Med. **37**(2), 161–171 (2005).
14. Y. Zhang, S. Song, C.-C. Fong, C.-H. Tsang, Z. Yang, and M. Yang, "cDNA microarray analysis of gene expression profiles in human fibroblast cells irradiated with red light," J. Invest. Dermatol. **120**(5), 849–857 (2003).
15. F. Ginani, D. M. Soares, M. P. E. V. Barreto, and C. A. G. Barboza, "Effect of low-level laser therapy on mesenchymal stem cell proliferation: a systematic review," Lasers Med. Sci. **30**(8), 2189–2194 (2015).
16. D. F. Wilson, "Oxidative phosphorylation: regulation and role in cellular and tissue metabolism," The J. Physiol. **595**(23), 7023–7038 (2017).
17. K. Alhallak, L. G. Rebello, T. J. Muldoon, K. P. Quinn, and N. Rajaram, "Optical redox ratio identifies metastatic potential-dependent changes in breast cancer cell metabolism," Biomed. Opt. Express **7**(11), 4364–4374 (2016).
18. W. Jones and K. Bianchi, "Aerobic glycolysis: beyond proliferation," Frontiers in Immunology **6**, 227 (2015).

Biomedical Optics EXPRESS

19. S. Papa, P. L. Martino, G. Capitanio, A. Gaballo, D. De Rasmo, A. Signorile, and V. Petruzzella, "The oxidative phosphorylation system in mammalian mitochondria," in *Advances in Mitochondrial Medicine*, vol. 942 R. Scatena, P. Bottoni, and B. Giardina, eds. (Springer Netherlands Dordrecht, 2012), pp. 3–37.
20. Z. Liu, D. Pouli, C. A. Alonzo, A. Varone, S. Karaliota, K. P. Quinn, K. Münger, K. P. Karalis, and I. Georgakoudi, "Mapping metabolic changes by noninvasive, multiparametric, high-resolution imaging using endogenous contrast," Sci. Adv. **4**(3), eaap9302 (2018).
21. O. I. Kolenc and K. P. Quinn, "Evaluating Cell Metabolism Through Autofluorescence Imaging of NAD(P)H and FAD," Antioxidants & Redox Signaling (2018).
22. C. Stringari, L. Abdeladim, G. Malkinson, P. Mahou, X. Solinas, I. Lamarre, S. Brizion, J.-B. Galey, W. Supatto, R. Legouis, A.-M. Pena, and E. Beaurepaire, "Multicolor two-photon imaging of endogenous fluorophores in living tissues by wavelength mixing," Sci. Rep. **7**(1), 3792 (2017).
23. M. Potter, E. Newport, and K. J. Morten, "The Warburg effect: 80 years on," Biochem. Soc. Trans. **44**(5), 1499–1505 (2016).
24. M. V. Liberti and J. W. Locasale, "The Warburg effect: how does it benefit cancer cells?" Trends Biochem. Sci. **41**(3), 211–218 (2016).
25. V. S. LeBleu, J. T. O'Connell, K. N. Gonzalez Herrera, H. Wikman, K. Pantel, M. C. Haigis, F. M. de Carvalho, A. Damascena, L. T. Domingos Chinen, R. M. Rocha, J. M. Asara, and R. Kalluri, "PGC-1α mediates mitochondrial biogenesis and oxidative phosphorylation in cancer cells to promote metastasis," Nat. Cell Biol. **16**(10), 992–1003 (2014).
26. X. Lu, B. Bennet, E. Mu, J. Rabinowitz, and Y. Kang, "Metabolomic changes accompanying transformation and acquisition of metastatic potential in a syngeneic mouse mammary tumor model," J. Biol. Chem. **285**(13), 9317–9321 (2010).
27. P. E. Porporato, V. L. Payen, J. Perez-Escuredo, C. J. De Saedeleer, P. Danhier, T. Copetti, S. Dhup, M. Tardy, T. Vazeille, C. Bouzin, O. Feron, C. Michiels, B. Gallez, and P. Sonveaux, "A mitochondrial switch promotes tumor metastasis," Cell Rep. **8**(3), 754–766 (2014).
28. R. Sethupathi, K. Gurushankar, and N. Krishnakumar, "Optical redox ratio differentiates early tissue transformations in DMBA-induced hamster oral carcinogenesis based on autofluorescence spectroscopy coupled with multivariate analysis," Laser Phys. **26**(11), 116202 (2016).
29. E. C. Lins, C. F. Oliveira, O. C. Guimaraes, C. A. d. S. Costa, C. Kurachi, and V. S. Bagnato, "A novel 785-nm laser diode-based system for standardization of cell culture irradiation," Photomed. Laser Surg. **31**(10), 466–473 (2013).
30. W. Denk, J. H. Strickler, and W. W. Webb, "Two-photon laser scanning fluorescence microscopy," Science **248**(4951), 73–76 (1990).
31. O. Warburg, "The metabolism of carcinoma cells," J. Cancer Res. **9**(1), 148–163 (1925).
32. M. Yamaura, M. Yao, I. Yaroslavsky, R. Cohen, M. Smotrich, and I. E. Kochevar, "Low level light effects on inflammatory cytokine production by rheumatoid arthritis synoviocytes," Lasers Surg. Med. **41**(4), 282–290 (2009).
33. M. E. de Abreu Chaves, A. R. de Araujo, A. C. C. Piancastelli, and M. Pinotti, "Effects of low-power light therapy on wound healing: LASER x LED," An. Bras. Dermatol. **89**(4), 616–623 (2014).
34. S. George, M. R. Hamblin, and H. Abrahamse, "Effect of red light and near infrared laser on the generation of reactive oxygen species in primary dermal fibroblasts," J. Photochem. Photobiol., B **188**, 60–68 (2018).
35. T. I. Karu, L. V. Pyatibrat, and N. I. Afanasyeva, "Cellular effects of low power laser therapy can be mediated by nitric oxide," Lasers Surg. Med. **36**(4), 307–314 (2005).
36. S. Sonis, "Could the impact of photobiomodulation on tumor response to radiation be effected by tumor heterogeneity?" Supportive Care in Cancer **28**, 423–424 (2019).
37. M. M. Schubert, F. P. Eduardo, K. A. Guthrie, J.-C. Franquin, R.-J. J. Bensadoun, C. A. Migliorati, C. M. E. Lloid, C. P. Eduardo, N.-F. Walter, M. M. Marques, and M. Hamdi, "A phase III randomized double-blind placebo-controlled clinical trial to determine the efficacy of low level laser therapy for the prevention of oral mucositis in patients undergoing hematopoietic cell transplantation," Support. Care Cancer **15**(10), 1145–1154 (2007).
38. G. Jaguar, J. Prado, I. Nishimoto, M. Pinheiro, D. De Castro Jr, D. Da Cruz Perez, and F. Alves, "Low-energy laser therapy for prevention of oral mucositis in hematopoietic stem cell transplantation," Oral Dis. **13**(6), 538–543 (2007).
39. L. Hu, N. Wang, E. Cardona, and A. J. Walsh, "Fluorescence intensity and lifetime redox ratios detect metabolic perturbations in t cells," Biomed. Opt. Express **11**(10), 5674–5688 (2020).
40. J. M. Levitt, A. Baldwin, A. Papadakis, S. Puri, J. Xylas, K. Munger, and I. Georgakoudi, "Intrinsic fluorescence and redox changes associated with apoptosis of primary human epithelial cells," J. Biomed. Opt. **11**(6), 064012 (2006).
41. P. G. B. Heymann, K. S. E. Henkenius, T. Ziebart, A. Braun, K. Hirthammer, F. Halling, A. Neff, and R. Mandic, "Modulation of tumor cell metabolism by laser photochemotherapy with cisplatin or zoledronic acid in vitro," Anticancer Res. **38**, 1291–1301 (2018).
42. L. Z. Li, R. Zhou, H. N. Xu, L. Moon, T. Zhong, E. J. Kim, H. Qiao, R. Reddy, D. Leeper, B. Chance, and J. D. Glickson, "Quantitative magnetic resonance and optical imaging biomarkers of melanoma metastatic potential," Proc. Natl. Acad. Sci. **106**(16), 6608–6613 (2009).
43. K. W. Engel, I. Khan, and P. R. Arany, "Cell lineage responses to photobiomodulation therapy," J. Biophotonics **9**(11-12), 1148–1156 (2016).

Biomedical Optics EXPRESS

44. M. Lunova, B. Smolková, M. Uzhytchak, K. Ž. Janoušková, M. Jirsa, D. Egorova, A. Kulikov, S. Kubinova, A. Dejneka, and O. Lunov, "Light-induced modulation of the mitochondrial respiratory chain activity: possibilities and limitations," Cell. Mol. Life Sci. **77**(14), 2815–2838 (2020).
45. A. Lynnyk, M. Lunova, M. Jirsa, D. Egorova, A. Kulikov Sarka Kubinova, O. Lunov, and A. Dejneka, "Manipulating the mitochondria activity in human hepatic cell line Huh7 by low-power laser irradiation," Biomed. Opt. Express **9**(3), 1283–1300 (2018).
46. A. C.-H. Chen, P. R. Arany, Y.-Y. Huang, E. M. Tomkinson, S. K. Sharma, G. B. Kharkwal, T. Saleem, D. Mooney, F. E. Yull, T. S. Blackwell, and M. R. Hamblin, "Low-level laser therapy activates nf-kb via generation of reactive oxygen species in mouse embryonic fibroblasts," PLoS One **6**, e22453 (2011).
47. M. R. Hamblin, S. T. Nelson, and J. R. Strahan, "Photobiomodulation and cancer: what is the truth?" Photomed. Laser Surg. **36**(5), 241–245 (2018).
48. R. D. Volker Hans Schartinger and Oliver GalvanHerbert, "Differential responses of fibroblasts, non-neoplastic epithelial cells, and oral carcinoma cells to low-level laser therapy," Support. Care Cancer **20**(3), 523–529 (2012).
49. F. F. Sperandio, F. S. Giudice, L. Correa, D. S. P. Jr., M. R. Hamblin, and S. C. de Sousa, "Low-level laser therapy can produce increased aggressiveness of dysplastic and oral cancer cell lines by modulation of akt/mtor signaling pathway," J. Biophotonics **6**, 839–847 (2013).
50. C. M. G. de Faria, H. Ciol, V. S. Bagnato, and S. Pratavieira, "Photobiomodulation effects on cell metabolism," figshare (2021) https://doi.org/10.6084/m9.figshare.13667411.